

Forced Convective and Nucleate Flow Boiling Heat Transfer to Alumina Nanofluids

Mohammad Mohsen Sarafraz / Faramarz Hormozi

RESEARCH ARTICLE

RECEIVED 15 JULY 2013; ACCEPTED AFTER REVISION 18 NOVEMBER 2013

Abstract

A large number of experiments have been performed to quantify the forced convective and nucleate flow boiling heat transfer coefficient of Al_2O_3 water based nanofluid. The employed test loop provides conditions to investigate the influence of operating parameters such as heat flux, flow mass flux and volumetric concentration of nanofluids (0.5, 1 and 1.5%). Results demonstrate that two heat transfer regions are observed namely forced convective and nucleate boiling region. Investigating on the operating parameters illustrated that with increasing the heat flux and flow rate of nanofluid, heat transfer coefficient of nanofluid dramatically increases. In contrast, with increasing the volumetric concentration of nanofluid, controversial condition is observed such that increases the heat transfer coefficient in forced convective region is reported while reduction of heat transfer coefficient is seen for nucleate boiling zone. Obtained results were then compared to Chen and also Gungor-Winterton well-known correlations. Results of this comparison show that experimental data are in a good agreement with those of obtained by correlations.

Keywords

nanofluid · Al_2O_3 · forced convective · nucleate boiling · Chen type model · Gungor-Winterton

Acknowledgement

Authors of this work tend to dedicate this article to Imam Hussein and Imam Mahdi and also appreciate Semnan State University for their financial supports and Islamic Azad University of Mahshahr for providing the alumina nanofluids. They also appreciate Khorramshahr University of marine sciences for their facilities.

Mohammad Mohsen Sarafraz

Faculty of Chemical, Petroleum and Gas Engineering,
Semnan University, Semnan, Iran
e-mail: mohadamohsensarafraz@gmail.com

Faramarz Hormozi

Faculty of Chemical, Petroleum and Gas Engineering,
Semnan University, Semnan, Iran

1 Introduction

Fluid heating and cooling play important roles in many industries including nuclear power plants, power cycles, power stations, production processes, transportation and electronics. Most applicable coolant, such as water, Ethylene Glycol and engine oil, have limited capabilities in term of thermal properties, which in turn, may impose severe restrictions in many thermal applications. Always, despite considerable research and efforts deployed, a clear and urgent need does exist to date to develop new strategies in order to improve the effective thermal behaviors of these fluids. On the other hand, most solids, in particular metals have thermal conductivities much higher comparing to that of liquids. Hence, one can then expect that fluid containing solid particles may significantly increase its conductivity [1]. Solid particles of the nominal size 1–100 nm are called nanoparticles, and low-concentration dispersions of such particles in a base fluid are called nanofluids. Nanofluids are known to apply a significant increase in thermal conductivity over that of the base fluid [2-6]. Also, as the particles are ultra-fine and at low concentrations, they probably overcome the problems of sedimentation. In fact, nanofluids have unprecedented stability of suspended nanoparticles were proven to be having anomalous thermal conductivity even with small volume fraction of the nanoparticles (dilute nanofluids) [7]. By suspending nanoparticles in heating or cooling fluids, the heat transfer performance of the fluid can be significantly improved. The main reasons may be listed as follows [8]:

- The suspended nanoparticles lead the surface area to be released and the heat capacity of the fluid to be enhanced.
- The suspended nanoparticles increase the thermal conductivity of the fluid.
- The interaction and collision among particles, fluid and the flow passage surface are intensified.
- Nanoparticles after depositing on the heating section change the surface characteristics and wettability of surface.

Forced convective and Boiling heat transfer continue to be a subject of ongoing researches because of their potential to remove large amounts of heat at low temperature difference and a lack of validated models. Early studies of application of

nanofluids in flow and pool boiling have mainly focused on critical heat flux and surface characteristics of a heating section as well as thermal conductivity enhancement and the parameters that govern this behavior [9-15]. Following literature briefly represents some recent works conducted on forced convective and flow boiling heat transfer of nanofluid.

2 State-of-the-art

Many investigations [16-17] have been conducted on forced and flow boiling heat transfer coefficient of nanofluids but following literature represents some of the latest researches about the convective and boiling heat transfer. As an example, an experimental study on the forced convective heat transfer and flow characteristics of TiO₂/water nanofluids under turbulent flow conditions has been reported by Duangthongsuk and Wongwisues [18]. A horizontal double-tube counter flow heat exchanger is used in their study. They observed a slightly higher (6–11%) heat transfer coefficient for nanofluid compared to pure water. The heat transfer coefficient increases with increasing mass flow rate of the hot water as well as nanofluid. Recently, Sarafraz et al. conducted some experimental investigations on pool boiling heat transfer of nanofluids around the horizontal cylinder [19,20]. Also, among very few studies on flow boiling of nanofluids, Kim et al. [9] represented about 50% enhancement in flow boiling Critical Heat Flux (CHF) for Al₂O₃/water nanofluids flowing through a vertical stainless steel tube. Very recently, Henderson et al. [21] studied refrigerant-based SiO₂ and CuO-nanofluids in flow boiling experiments in horizontal copper tube. They found that while the Boiling Heat Transfer Coefficient (BHTC) of SiO₂/R-134a nanofluid decreases up to 55% in comparison to pure R-134a, the BHTC increases more than 100% for CuO-laden nanofluid over base fluid, i.e. mixture of R-134a and polyolester oil (PO). Tsai et al. studied about the effect of structural character of nanoparticles on heat pipe thermal performance and concluded that the thermal resistance of the heat pipes with nanofluids was lower than that of distilled water [22]. Ding and Wen illustrated that the nanoparticles migration due to spatial gradient in viscosity and shear rate, as well as the Brownian motion has a significant implication to heat transfer [23]. Nanofluid phase change was investigated by Das et al. [24]. They observed boiling performance deterioration for nanofluids.

Objective of this work is to represent a set of experimental data related to the flow boiling heat transfer coefficient of Al₂O₃/water nanofluid and investigate the influence of some operating parameters such as heat flux, fluid flow rate and volumetric concentration (vol. %) of particles in base fluid on forced convective and flow boiling heat transfer coefficient of Al₂O₃ water based nanofluids. Also, a rough comparison is made between the experimental data and two well-known correlations (Chen model and Gungor-Winterton). This comparison represents the good agreement between experimental data and those computed using above-mentioned correlations.

3 Experimental

3.1 Preparation of nanofluids

In the present work, different volumetric concentrations of nanofluids are prepared using two step methods. The Al₂O₃ nanoparticles (45-55nm, mostly 50nm, PlasmaChem GmbH, Germany) uniformly dispersed into the base fluid for making a stable nanofluid. In the present work, deionized water is considered as base fluid. Briefly, the preparation steps are:

- I. Weight the mass of Al₂O₃ with digital electronic balance (A&D EK Series Portable Balances, EK-1200i).
- II. Initially, the weighted Al₂O₃ nanoparticle was added into the weighted deionized water while it was agitated in a flask. The magnetic motorized stirrer (Hanna instruments Co.) was employed to agitate the nanoparticle inside the base fluid.
- III. UP400S ultrasonic Hielscher GmbH (400W / 24 kHz) is used to disperse the nanoparticles into the water uniformly.

In the present work, nanofluids with volumetric concentrations of 0.5%, 1% and 1.5% is prepared using the 45-50nm (claimed by manufacturer) Al₂O₃ as nanoparticle and deionized water as based fluid. Also, particle size examinations as well as XRD test of solid particles were performed to see how much the claims of manufacturer about the sizes and quality of nanoparticles are in real true. As can be seen in Fig. 1, maximum size counts are related to 45-50nm particles. Fig. 2 depicts the SEM image of Al₂O₃ nanoparticles. XRD pattern (Fig. 3) also depicts the single-phase Al₂O₃ with a monoclinic structure which implies on this fact that there is no impurity other than Al₂O₃ nanoparticles and no significant peaks of impurities are found in XRD pattern. The peaks are broad due to the nano-size Effect.

Schematic of the main components of the close loop experimental facility constructed in the present study is shown in Fig. 4. The working fluid enters the loop from a main tank through the isolated pipes and is continuously circulated by a centerfugal pump (DAB Co.). Duo to the importance of flow rate of fluid in flow boiling heat transfer, a Netflix ultrasonic flow meter is also installed in trajectory line of fluid to measure the flow rate with the least possible uncertainty. Also, a rotameter is installed at the outlet line of condenser to validate the flow rate values measured by ultrasonic device. The fluid temperature was measured by two PT-100 thermometers installed in two thermo-well located just before and after the annular section. The complete cylinder was made from stainless steel 316a. Thermometer voltages, current and voltage drop from the test heater were all measured and processed with a data acquisition system in conjunction with a PID temperature controller. The test section shown in Fig. 4 consists of an electrically heated cylindrical DC bolt heater (manufactured by Cetal Co.) with a stainless steel surface, which is mounted concentrically within

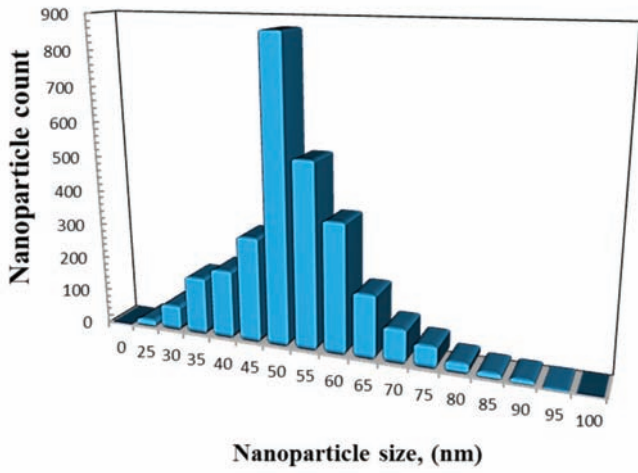


Fig. 1. Particle size distribution of Al_2O_3 nanoparticles

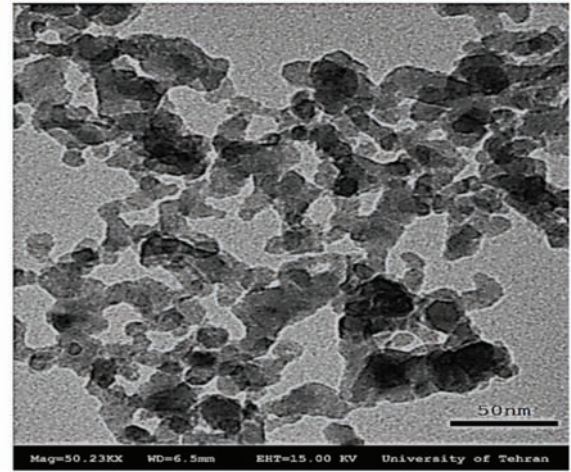


Fig. 2. TEM image of Al_2O_3 nanofluid; vol. %=0.5; uniform dispersion of alumina nanofluid can be seen

the surrounding pipe. The dimensions of the test section are: diameter of heating rod, 22 mm; annular gap diameter (hydraulic diameter) 30 mm; the length of the pyrex tube is 400 mm; the length of stainless steel rod, 300 mm; the length of heated section, 140 mm which means that just the first 140 mm of stainless steel is heated uniformly and radially by the heater. The axial heat transfer through the rod can be ignored according to the insulation of the both ends of the heater. The heat flux and wall temperature can be as high as $190,000 \text{ W.m}^{-2}$ and 163°C , respectively. The local wall temperatures have been measured with four stainless steel sheathed K-type thermocouples which have been installed close to the heat transfer surface.

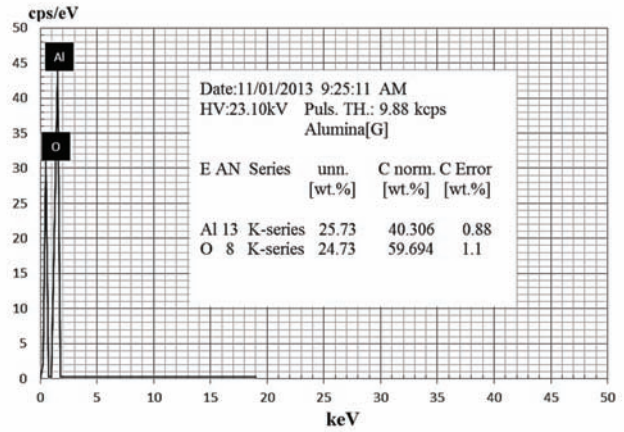


Fig. 3. XRD results of Al_2O_3 solid nanoparticles

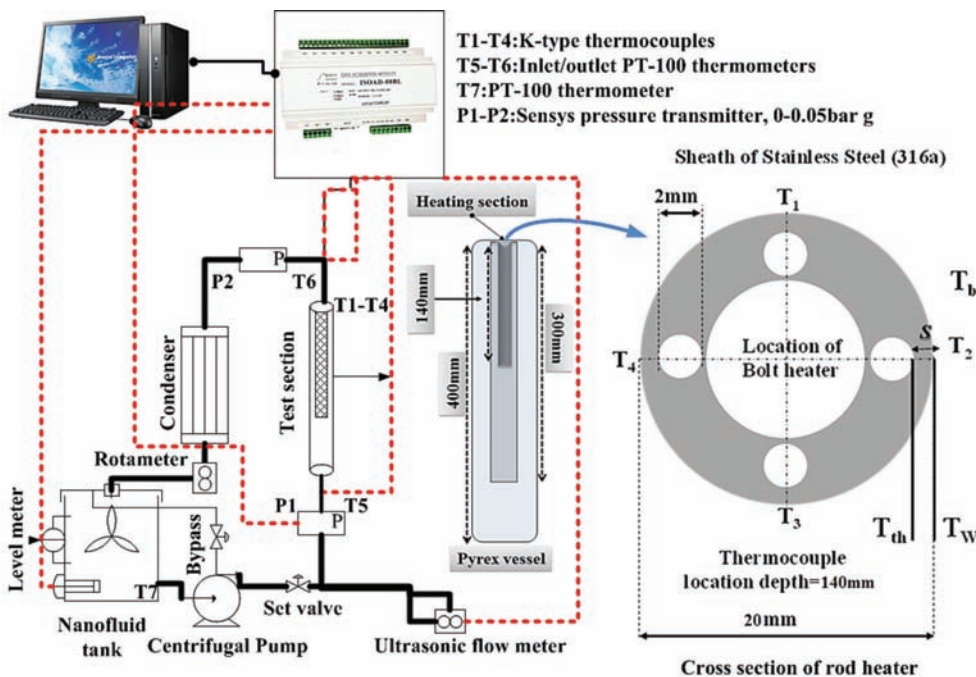


Fig. 4. A scheme of test loop

The temperature drop between the thermocouples location and the heat transfer surface can be calculated from:

$$T_w = T_{th} - \dot{q} \frac{S}{\lambda_w} \quad (1)$$

The ratio between the distance of the thermometers from the surface and the thermal conductivity of the tube material (s/λ_w) was determined for each K-type thermocouple by calibration using Wilson plot technique [25]. The average temperature difference for each test section was the arithmetic average of the four thermometers readings around the rod circumference. The average of 10 voltage readings was used to determine the difference between the wall and bulk temperature for each thermometer. All the K-type thermocouples were thoroughly calibrated using a constant temperature water bath, and their accuracy has been estimated to $\pm 0.3K$. The local heat transfer coefficient α is then calculated from:

$$\alpha = \frac{\dot{q}}{(T_w - T_b)_{av.}} = \frac{V \times I}{(T_w - T_b)_{av.}} \quad (2)$$

V is voltage (V) and I is current (A). Voltage and current of the system was measured using Fluke multi meter with $\pm 1\%$ of reading. Also, to minimize the thermal contact resistance, high quality silicone paste was injected into the thermocouple wells. To avoid possible heat loss, main tank circumferences were heavily insulated using industrial glass wool. To control the fluctuations due to the alternative current, a regular DC power supply was also employed to supply the needed voltage to central heater. Likewise, to visualize the flow and boiling phenomenon and record the proper images, annulus was made of the Pyrex glass.

3.2 Uncertainty analysis

The uncertainties of the experimental results are analyzed by the procedures proposed by Kline and McClintock [26]. The method is based on careful specifications of the uncertainties in the various primary experimental measurements. The heat transfer coefficient can be obtained using Eq. (9):

$$\alpha = \frac{\rho \dot{V} C_{p,nf} (T_{out} - T_{in})}{A \cdot (T_w - T_b)_{av.}} \quad (9)$$

As seen from Eq. (9), the uncertainty in the measurement of the heat transfer coefficient can be related to the errors in the measurements of volume flow rate, hydraulic diameter, and all the temperatures as follows.

$$\alpha = f\left(\dot{V}, A_h, (T_{out} - T_{in}), (T_w - T_b)\right) \quad (10)$$

$$\begin{aligned} \partial\alpha = & \left[\left(\left[\frac{\partial\alpha}{\partial V} \right] \delta V \right)^2 + \left(\left[\frac{\partial\alpha}{\partial A} \right] \delta V \right)^2 \right. \\ & + \left. \left(\left[\frac{\partial\alpha}{\partial (T_{out} - T_{in})} \right] \delta (T_{out} - T_{in}) \right)^2 \right. \\ & + \left. \left(\left[\frac{\partial\alpha}{\partial (T_w - T_b)} \right] \delta (T_w - T_b) \right)^2 \right]^{0.5} \end{aligned} \quad (11)$$

Noticeably, A_h is hydraulic cross section area based on the hydraulic diameter,

$$d_h = \frac{4A}{P};$$

where (A is the cross sectional area and P is the wetted perimeter of the cross-section. For annulus system $d_h = d_2 - d_1$. In this work, d_2 (diameter of glass Pyrex) is 50mm and d_1 (diameter of stainless steel rod) is 20mm. therefore; hydraulic diameter would be 30mm. According to the above uncertainty analysis, the uncertainty in the measurement of the heat transfer coefficient is 16.23%. The detailed results from the present uncertainty analysis for the experiments conducted here are summarized in Table 1. The main source of uncertainty is due to the temperature measurement and its related devices.

3.3 Thermo-physical properties of nanofluids

In this work, it is assumed that Al_2O_3 nanoparticles are well dispersed within the base fluid due to using the ultrasonic device and magnetic stirrer. Therefore, following correlations can be used for estimating the physical properties of nanofluids [27-29]. In this paper, the following correlations are used to calculate the density, viscosity and the specific heat of Al_2O_3 /water nanofluid as follows in Table 2.

4 Results and discussions

In this section, influence of different operating parameters on forced convective and nucleate flow boiling heat transfer coefficient of nanofluids are discussed. Also, deionized water is considered as a reference fluid and results of experiments are compared to deionized water.

4.1 Effect of heat flux

Conveniently, influence of heat flux on forced convective and flow boiling heat transfer coefficient is shown in terms of heat flux versus heat transfer coefficient. According to previous studies [22,30,31] in flow boiling heat transfer two distinguishable heat transfer region is observed. The first is forced convective heat transfer controlled and the second is nucleate boiling heat transfer controlled. Fig. 5 depicts the forced

Tab. 1. Summary of the uncertainty analysis

Parameter	Uncertainty
Length, width and thickness, (m)	$\pm 5 \times 10^{-5}$
Temperature, (K)	$\pm 0.3K$
Water flow rate, (lit. min ⁻¹)	$\pm 1.5\%$ of readings
Voltage, (V)	$\pm 1\%$ of readings
Current, (A)	$\pm 0.02\%$ of readings
Cylinder side area, (m ²)	$\pm 4 \times 10^{-8}$
Flow boiling heat transfer coefficient, (W/m ² .K)	$\pm 16.23\%$

convective and flow boiling heat transfer regions. As can be seen, for both heat transfer region, with increasing the heat flux, heat transfer coefficient obviously increases.

Fig.6 represents the bubble formation during the flow boiling of deionized water. All concentrations of Al₂O₃ nanofluids are not transparent. Therefore, images related to the deionized water are represented. As can be seen, with increasing the heat flux, rate of bubble formation strongly increases. Noticeably, increasing the heat flux leads to the surface temperature to be increased and consequently, rate of bubble generation increases too. Likewise, as can be seen in Fig. 6, numbers of nucleate active sites are dramatically increased.

4.2 Effect of fluid mass flux

Fluid flow rate (volumetric or mass flux) has a strong influence on flow boiling heat transfer coefficient in both heat transfer regions. Experimental results reveal a significant increase of heat transfer coefficient when fluid mass flux increases. Fig. 7 typically represents the effect of fluid flow rate on flow boiling heat transfer coefficient of Al₂O₃ water based nanofluids.

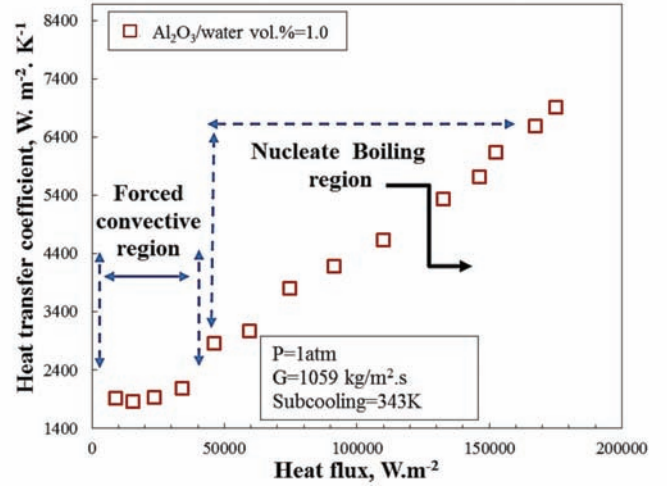


Fig. 5. Experimental flow boiling heat transfer coefficient of Al₂O₃ water based nanofluid

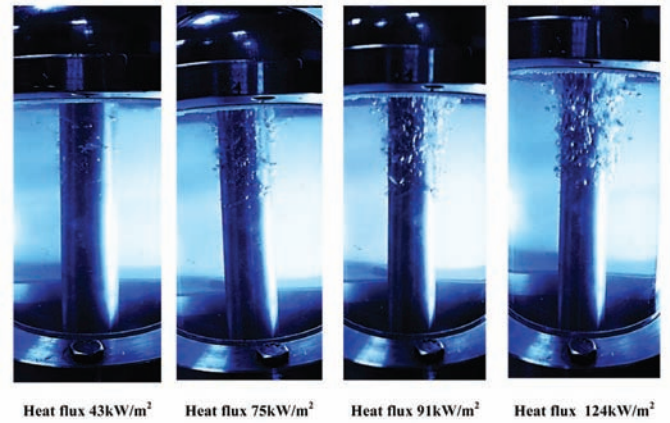


Fig. 6. Bubble formation of deionized water as base fluid in flow boiling

Tab. 2. Correlations for predicting the thermo-physical properties of nanofluids

Physical properties	Correlation	reference
Density	$\rho_{nf} = \varphi\rho_p + (1-\varphi)\rho_{bf}$	29
Heat capacity	$C_{pnf} = (1-\varphi)\left(\frac{\rho_{bf}}{\rho_{nf}}\right)C_{pmf} + \varphi\left(\frac{\rho_p}{\rho_{nf}}\right)C_{pp}$	29
Viscosity	$\mu_{nf} = A\left(\frac{1}{T}\right) - B$ $A = 20587\varphi^2 + 15857\varphi + 1078.3, B = -107.12\varphi^2 + 53.548\varphi + 2.8715$	29
Thermal conductivity	$K_{nf} = \frac{K_p + (n-1)K_{bf} - \varphi(n-1)(K_{bf} - K_p)}{K_p + (n-1)K_{bf} + \varphi(K_{bf} - K_p)} K_{bf} + 5 \times 10^4 \beta \varphi \rho_{bf} C_{pbf} \cdot \Pi$ $\Pi = \sqrt{\frac{\kappa T}{\rho_p d_p}} f(T, \varphi)$ $f(\varphi, T) = 2.8217 \times 10^{-2} \varphi + 3.917 \times 10^{-3} \left(\frac{T}{T_0}\right) - 3.0669 \times 10^{-2} \varphi - 3.911 \times 10^{-3}$ <i>For CuO nanoparticle: $\beta = 9.881 \times (100\varphi)^{-0.9446}$ $n = \frac{3}{\phi}$, ϕ: Sphericity of nanoparticles [34]</i>	29

4.3 Effect of concentration of nanofluid

Effect of concentration of nanofluid on heat transfer coefficient in flow boiling of $\text{Al}_2\text{O}_3/\text{water}$ is one of the matters of controversial. When concentration of nanofluid increases, in forced convective region, heat transfer coefficients slightly increase while in nucleate boiling zone, deterioration of heat transfer coefficient is clearly seen. Due to the sedimentation of nanoparticles around the heating section and coating appears on the surface, surface heat transfer resistance increases and becomes isolated against the heat transfer. On the other hand surface characteristic is changed and wettability of surface is also changed and leads the bubbles to cover the heating surface which leads the heat transfer to decrease. Fig. 8a illustrates the influence of concentration of nanofluids on flow boiling heat transfer coefficient. To evaluate the influence of concentration on flow boiling heat transfer coefficient of alumina nanofluids, enhancement ratio is employed which can be obtained by

$$d_h = \frac{4A}{p},$$

is the heat transfer coefficient in presence of nanoparticles and α_{bf} is the heat transfer of base fluid without the nanoparticles. As can be seen in Fig. 8b, in force convective region, enhancement ratio increases while, in nucleate boiling zone, reduction of enhancement ratio is significantly seen especially, when concentration of nanofluids increases. Reduction of enhancement ratio in nucleate boiling region is due to the scale formation of nanofluids around the heating section and changes of bubble formation around the heating section. Since, rate of bubble formation increases due to the wettability of surface, bubbles cover the heating section and isolate it which leads the transferred heat to be reduced. In contrast, enhancement of thermal conductivity of nanofluids in convective region is the main reason of enhancement of heat transfer coefficient in this zone. Fig. 8b shows the enhancement ratio in force convective and nucleate boiling regions for alumina nanofluid in flow boiling phenomenon.

4.4 Comparison with well-known correlations

To investigate the accuracy of experimental data, these results are compared with those obtained by two well-known correlations namely: Chen model [32] and Gungor-Winterton [33] correlation. Table 3 shows the used correlations. These correlations are including with some thermo-physical properties such as density, thermal conductivity, viscosity and heat capacity. These properties can be estimated using table 2 correlations.

Results of comparison illustrated that experimental data represents the good agreement with those obtained by correlations. As can be seen in Figs. (9-10) the Chen correlation predicts the reasonable values with Absolute Average Deviation, A.A.D% of 20%. For Gungor-Winterton the average deviation was 30% which shows the fair agreement with those of experimentally

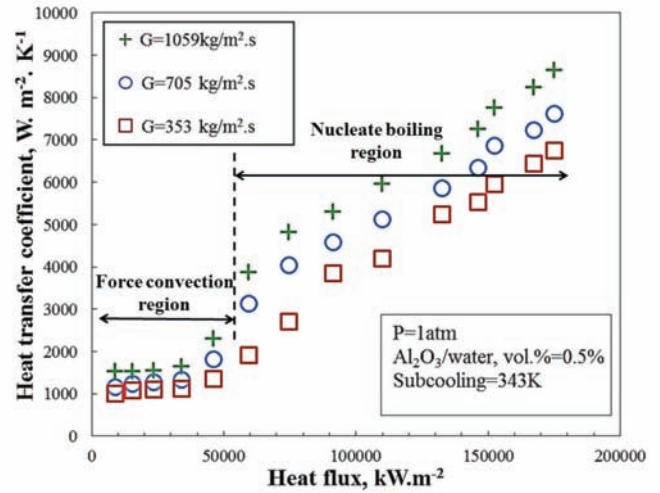


Fig. 7. Influence of mass flux on heat transfer coefficient of $\text{Al}_2\text{O}_3/\text{water}$ at volumetric concentration of 0.5%

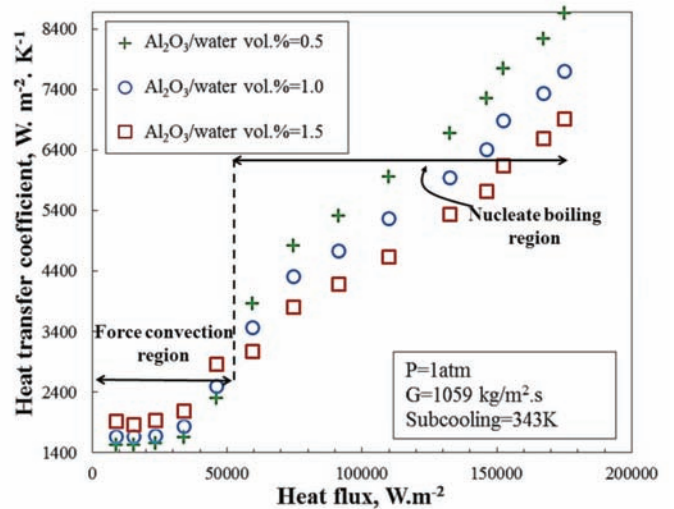


Fig. 8a. Influence of concentration of nanofluids on flow boiling heat transfer coefficient of Al_2O_3 -water nanofluid; increase of heat transfer coefficient of forced convective region and decrease of heat transfer coefficient of nucleate boiling zone is clearly observed.

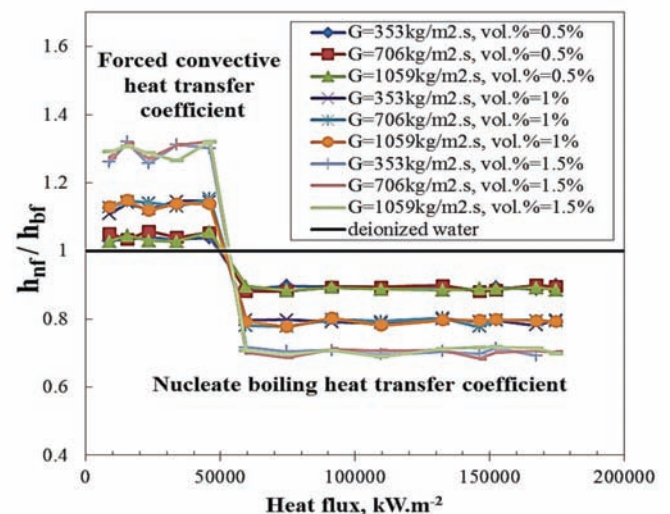


Fig. 8b. Increase/decrease of flow boiling heat transfer coefficient in forced convective and nucleate boiling heat transfer regions respectively.

Tab. 3. Predictive correlations for flow boiling heat transfer coefficient

Author	Eq. number
Chen type model: Eq. s (12-21)	
$\alpha_{fb} = S.\alpha_{nb} + F.\alpha_{fc}$	12
$F = \begin{cases} 1 & \text{if } \frac{1}{X_{tt}} \leq 0.1 \\ 2.35 \left(\frac{1}{X_{tt}} + 0.213 \right)^{0.736} & \text{if } \frac{1}{X_{tt}} \geq 0.1 \end{cases}$	13
$S = \frac{1}{1 + 2.53 \times 10^{-6} \text{Re}^{1.17}}$	14
$X_{tt} = \left(\frac{1 - \dot{x}}{\dot{x}} \right)^{0.9} \left(\frac{\rho_v}{\rho_l} \right)^{0.5} \left(\frac{\mu}{\mu_v} \right)^{0.1}$	15
$N_{Re} = \frac{\dot{m}(1 - \dot{x})d_h}{\mu} F^{1.25}$	16
$\dot{x} = N_{ph} - N_{ph0} \exp\left(\frac{N_{ph}}{N_{ph_n}} - 1\right)$	17
$N_{ph_0} = \frac{-C_p(T_{sat} - T_b)}{\Delta H_v}$	18
$N_{ph} = \frac{-N_{Bo}}{\sqrt{\left(\frac{455}{N_{pe_l}}\right)^2 + 0.0065^2}}$	19
$Bo = \frac{\dot{q}}{\dot{m} \cdot \Delta H_v}$	20
$Pe = \frac{\dot{m} C_p d_h}{k}$	21

Author	Eq. number
Gungor-Winterton: Eq. s (22-25)	
$\alpha_{fb} = S.\alpha_{nb} + F.\alpha_{fc}$	22
$F = 1 + 2.4 \times 10^4 Bo^{1.16} + 1.23 \left[\frac{1}{X_{tt}} \right]^{0.86}$	23
$\alpha_{nb} = 55 P_r^{0.55} \cdot (-\log P_r)^{-0.55} \cdot M^{-0.5} \cdot q^{0.67}$	24
$\alpha_{fc} = 0.023 N_{Re}^{0.8} N_{Pr}^{0.4} \left(\frac{l}{d_h} \right)$	25

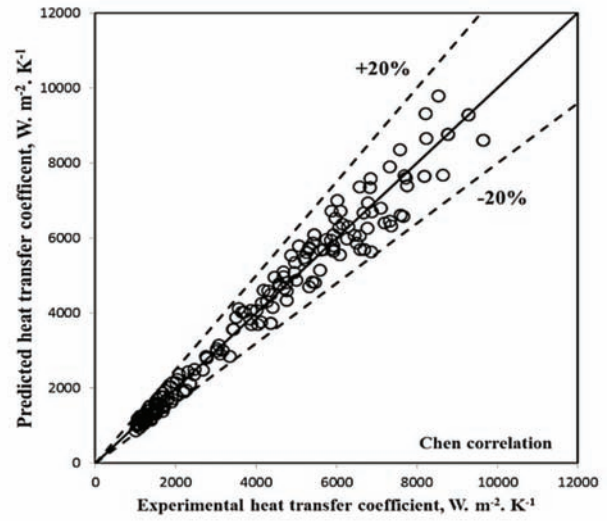


Fig. 9. Comparison between experimental results and obtained results by Chen correlation

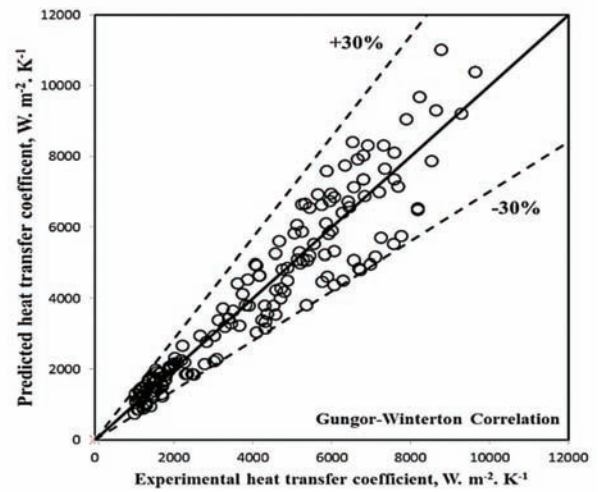


Fig. 10. Comparison between experimental results and obtained results by Gungor-Winterton correlation

obtained. Therefore, it is recommended to use the Chen type model for predicting the flow boiling heat transfer coefficient of dilute volumetric concentration of Al_2O_3 providing that the correlations of table 2 is used for estimating the thermo-physical properties involved.

5 Conclusions

Experimental investigation on flow boiling heat transfer coefficient of dilute Al_2O_3 water based nanofluid was conducted and following conclusions were made:

- According to experimental data, two distinguishable heat transfer regions are observed including the forced convective and nucleate boiling heat transfer regions.
- Heat flux and mass flux have a strong influence on heat transfer coefficient in both of heat transfer regions. With increasing the heat and mass flux, heat transfer coefficient dramatically increases.

- Concentration of nanofluid has a controversial effect on flow boiling heat transfer coefficient. With increasing the concentration of nanofluid, due to the deposition of particles around the heating section, heat transfer coefficient in nucleate boiling region decreases while in forced convective region heat transfer coefficient increases.
- It is recommended to use nanofluids to increase the heat transfer rate in forced convective regions, however using the nanofluid coolant in nucleate boiling region deteriorate the heat transfer coefficient.
- Chen correlation can be predict the heat transfer coefficient of nanofluids with A.A.D% of about 20% while Gungor-Winterton obtained a reasonable values with deviation about 30%.

Nomenclature

A	:cross section area, m^2
A_h	:Area calculated by hydraulic diameter, m^2
b	:distance, m
Bo	:boiling number
C_p	:heat capacity, $J.kg^{-1}.^{\circ}C^{-1}$
d_b	:bubble departing diameter, m
d_h	:hydraulic diameter, m, $D_h = \frac{4A}{P}$
f	:fanning friction number
F	:enhancement factor
G	:mass flux, $kg.m^{-2}.s^{-1}$
h	:specific enthalpy, $J.kg^{-1}$
ΔH_v	:heat of vaporization, $J.kg^{-1}$
K	:thermal conductivity, $W.m^{-1}.^{\circ}C^{-1}$
l_{th}	:heated length, m
l	:characteristic length, m
L	:heater length, m
M	:molecular weight, $kg.kmole^{-1}$
X	:Mole fraction
\dot{m}	:mass flow rate, $kg.s^{-1}$
N	:dimensionless groups, See Table 3
N_{ph}	:Phase change number
N_{Nu}	:Nusslet number
N_{Re}	:Reynolds number
N_{Bo}	:Boiling number
N_{Pe}	:Peclet number
N_{Pr}	:Prandtl number
ΔL	:characteristic length, m
P_r	:reduced pressure
P	:pressure, Pa

\bar{p}	:wetted perimeter of the cross-section
q	:heat, J
\dot{q}	:heat flux, $kW.m^{-2}$
R_a	:roughness, m
s	:distance between thermometer location and heat transfer surface, m
S	:suppression factor
T	:temperature, K
\dot{V}	:Water content in the membrane
x	:liquid mass or mole fraction
\dot{x}	:vapour mass fraction
X_{tt}	:Martinelli parameter
y	: vapor mass or mole fraction

Subscripts and superscripts

b	:bulk
bf	:base fluid
nf	:nanofluid
c	:critical
fb	:flow boiling
h	:hydraulic
in	:inlet
out	:outlet
l	:liquid
m	:mixture
n	:number of components
nb	:nucleate boiling
r	:reduced
Sat	:saturated
th	:thermometers
v	:vapor
w	:wall

Greek symbols

α	:heat transfer coefficient, $\text{W.m}^{-2}.\text{K}^{-1}$
ρ	:density, kg.m^{-3}
μ	:viscosity, $\text{kg.m}^{-1}.\text{s}^{-1}$
κ	:Boltzmann constant = 1.381×10^{-23} , J. K^{-1}
λ_w	:thermal conductivity of heating section, $\text{W.m}^{-1}.\text{K}^{-1}$
ϕ	:volume fraction
Δ	:difference
φ	:particle sphericity

Abbreviations

AAD%	:Absolute Average Deviation
ONB	:onset of nucleate boiling
Vol. %	:volumetric concentration in percent

Dimensionless groups

Bo	:boiling number = $\frac{\dot{q}}{\dot{m}.h_{fg}}$
Nu	:Nusslet number = $\frac{hd}{k}$
Pe	:peclet number = $\frac{\dot{m}C_p d_h}{k}$
Ph	:phase change number = $\frac{-N_{Bo}}{\sqrt{\left(\frac{455}{N_{pe1}}\right)^2 + 0.0065^2}}$
Pr	:Prandtl number = $\frac{c_p \mu}{k}$
Re	:Reynolds number = $\frac{\rho v d}{\mu}$

References

- 1 Maiga S. E. B., Palm S. J., Nguyen C. T., Roy G., Galanis N., *Heat transfer enhancement by using nanofluids in forced convection flows*. International Journal of Heat and Fluid Flow, 26(4), 530–546 (2005). DOI: [10.1016/j.ijheatfluidflow.2005.02.004](https://doi.org/10.1016/j.ijheatfluidflow.2005.02.004)
- 2 Cheng L., Liu L., *Boiling and two-phase flow phenomena of refrigerant-based nanofluids Fundamentals, applications and challenges*. International Journal of Refrigeration, 36(2), 421–446 (2013). DOI: [10.1016/j.jrefrig.2012.11.010](https://doi.org/10.1016/j.jrefrig.2012.11.010)
- 3 Choi S. U. S., Zhang Z. G., Yu W., Lockwood F. E., Grulke E. A., *Anomalous thermal conductivity enhancement in nanotube suspensions*. Applied Physics Letters, 79(14), 2252–2254 (2001). DOI: [10.1063/1.1408272](https://doi.org/10.1063/1.1408272)
- 4 Das S. K., Putra N., Roetzel W., *Pool boiling characteristics of nano-fluids*. International Journal of Heat and Mass Transfer, 46(5), 851–862 (2003).
- 5 Ding Y., Alias H., Wen D., Williams R. A., *Heat transfer of aqueous suspensions of carbon nanotubes (CNT nanofluids)*. International Journal of Heat and Mass Transfer, 49(1–2), 240–250 (2006). DOI: [10.1016/j.ijheatmasstransfer.2005.07.009](https://doi.org/10.1016/j.ijheatmasstransfer.2005.07.009)
- 6 He Y., Jin Y., Chen H., Ding Y., Cang D., Lu H., *Heat transfer and flow behavior of aqueous suspensions of TiO_2 nanoparticles (nanofluids) flowing upward through a vertical pipe*. International Journal of Heat and Mass Transfer, 50(11–12), 2272–2281 (2007). DOI: [10.1016/j.ijheatmasstransfer.2006.10.024](https://doi.org/10.1016/j.ijheatmasstransfer.2006.10.024)
- 7 Jung J., Oh H. S., Kwak H. Y., *Forced convective heat transfer of nanofluids in microchannels*. International Journal of Heat and Mass Transfer, 52(1–2), 466–472 (2009). DOI: [10.1016/j.ijheatmasstransfer.2008.03.033](https://doi.org/10.1016/j.ijheatmasstransfer.2008.03.033)
- 8 Xuan Y., Li Q., *Heat transfer enhancement of nanofluids*. International Journal of Heat and Fluid Flow, 21(1), 58–64 (2000).
- 9 Kim H., Kim J., Kim M. H., *Effect of nanoparticles on CHF enhancement in pool boiling of nano-fluids*. International Journal of Heat and Mass Transfer, 49(25–26), 5070–5074 (2006). DOI: [10.1016/j.ijheatmasstransfer.2006.07.019](https://doi.org/10.1016/j.ijheatmasstransfer.2006.07.019)
- 10 Kim S. J., Bang I. C., Buongiorno J., Hu L. W., *Effects of nanoparticle deposition on surface wettability influencing boiling heat transfer in nanofluids*. Applied Physics Letters, 89(15), 153107–153107-3 (2006). DOI: [10.1063/1.2360892](https://doi.org/10.1063/1.2360892)
- 11 Kim H. D., Kim J. B., Kim M. H., *Experimental studies on CHF characteristics of nano-fluids at pool boiling*. International Journal of Multiphase Flow, 33(7), 691–706 (2007). DOI: [10.1016/j.ijmultiphaseflow.2007.02.007](https://doi.org/10.1016/j.ijmultiphaseflow.2007.02.007)
- 12 Kim S. J., Bang I. C., Buongiorno J., Hu L. W., *Study of pool boiling and critical heat flux enhancement in nanofluids*. Bulletin of the Polish Academy Sciences Technical Sciences, 55(2), 211–216 (2007).
- 13 Kim S. J., McKrell T., Buongiorno J., Hu L. W., *Experimental study of flow critical heat flux in alumina–water; zinc-oxide–water and diamond–water nanofluids*. Journal of Heat Transfer, 131(4), (043204), 7 pages (2009). DOI: [10.1115/1.3072924](https://doi.org/10.1115/1.3072924)
- 14 Kim T. I., Jeong Y. H., Chang S. H., *An experimental study on CHF enhancement in flow boiling using Al_2O_3 nano-fluid*. International Journal of Heat and Mass Transfer, 53(5–6), 1015–1022 (2010). DOI: [10.1016/j.ijheatmasstransfer.2009.11.011](https://doi.org/10.1016/j.ijheatmasstransfer.2009.11.011)
- 15 Groeneveld D. C., *The 1995 look-up table for critical heat fluxes in tubes*. Nuclear Engineering and Design, 163(1–2), 1–23 (1996).
- 16 Murshed S. M., *A review of boiling and convective heat transfer with nanofluids*. Renewable Sustainable Energy Reviews, 15(5), 2342–2354 (2011). DOI: [10.1016/j.rser.2011.02.016](https://doi.org/10.1016/j.rser.2011.02.016)
- 17 Kakaç S., Pramuanjaroenki A., *Review of convective heat transfer enhancement with nanofluids*. International Journal of Heat and Mass Transfer, 52(13–14), 3187–3196 (2009). DOI: [10.1016/j.ijheatmasstransfer.2009.02.006](https://doi.org/10.1016/j.ijheatmasstransfer.2009.02.006)

- 18 Duangthongsuk W., Wongwises S., *Effect of thermo-physical properties models on the predicting of the convective heat transfer coefficient for low concentration nanofluid*. International Communications in Heat and Mass Transfer, 35(10), 1320-1326 (2008). DOI: [10.1016/j.icheatmasstransfer.2008.07.015](https://doi.org/10.1016/j.icheatmasstransfer.2008.07.015)
- 19 Sarafraz M. M., Peyghambarzadeh S. M., Alavi Fazel S. A., Vaeli N., *Nucleate pool boiling heat transfer of binary nano mixtures under atmospheric pressure around a smooth horizontal cylinder*. Periodica Polytechnica, Chemical Engineering, 57(1-2), 71-77 (2013). DOI: [10.3311/PPch.2173](https://doi.org/10.3311/PPch.2173)
- 20 Sarafraz M. M., Pyghambarzadeh S. M., *Nucleate Pool Boiling Heat Transfer to Al₂O₃-Water and TiO₂-Water Nanofluids on Horizontal Smooth Tubes with Dissimilar Homogeneous Materials*. Chemical and Biochemical Engineering Quarterly, 26(3), 199-206 (2012).
- 21 Henderson K., Park Y. G., Liu L., Jacobi A.M., *Flow-boiling heat transfer of R-134a based nanofluids in a horizontal tube*. International Journal of Heat and Mass Transfer, 53(5-6), 944-951 (2010). DOI: [10.1016/j.ijheatmasstransfer.2009.11.026](https://doi.org/10.1016/j.ijheatmasstransfer.2009.11.026)
- 22 Sarafraz M. M., Peyghambarzadeh S. M., *Experimental study on subcooled flow boiling heat transfer to water-diethylene glycol mixtures as a coolant inside a vertical annulus*. Experimental Thermal and Fluid Science, 50, 154-162 (2013). DOI: [10.1016/j.expthermflusci.2013.06.003](https://doi.org/10.1016/j.expthermflusci.2013.06.003)
- 23 Ding Y., Alias H., Wen D., Williams R. A., *Heat transfer of aqueous suspensions of carbon nanotubes (CNT nanofluids)*. International Journal of Heat and Mass Transfer, 49(1-2), 240-250 (2006). DOI: [10.1016/j.ijheatmasstransfer.2005.07.009](https://doi.org/10.1016/j.ijheatmasstransfer.2005.07.009)
- 24 Das S. K., Putra N., Roetzel W., *Pool boiling of nanofluids on horizontal narrow tubes*. International Journal of Multiphase Flow, 29(8), 1237-1247 (2003). DOI: [10.1016/S0301-9322\(03\)00105-8](https://doi.org/10.1016/S0301-9322(03)00105-8)
- 25 Seara J. F., Uhia F. J., Sieres J., *Laboratory practices with the Wilson plot method*. Experimental Heat Transfer: A Journal of Thermal Energy Generation, Transport, Storage, and Conversion, 20(2), 123-135 (2007). DOI: [10.1080/08916150601091415](https://doi.org/10.1080/08916150601091415)
- 26 Kline S. J., McClintock F. A., *Describing uncertainties in single-sample experiments*. Mechanical Engineering, 75(1), 3-12 (1953).
- 27 Wang X., Xu X., Choi S. U. S., *Thermal conductivity of nanoparticles fluid mixture*. Journal of Thermophysics and Heat Transfer, 13(4), 474-480 (1999). DOI: [10.2514/2.6486](https://doi.org/10.2514/2.6486)
- 28 Xuan Y., Roetzel W., *Conceptions for heat transfer correlation of nanofluids*. International Journal of Heat and Mass Transfer, 43(19), 3701-3707 (2000). DOI: [10.1016/S0017-9310\(99\)00369-5](https://doi.org/10.1016/S0017-9310(99)00369-5)
- 29 Peyghambarzadeh S. M., Hashemabadi S. H., Naraki M., Vermaahmoudi Y., *Experimental study of overall heat transfer coefficient in the application of dilute nanofluids in the car radiator*. Applied Thermal Engineering, 52(1), 8-16 (2013). DOI: [10.1016/j.applthermaleng.2012.11.013](https://doi.org/10.1016/j.applthermaleng.2012.11.013)
- 30 Peyghambarzadeh S. M., Sarafraz M. M., Vaeli N., Ameri E., Vatani A., Jamialahmadi, M., *Forced convective and subcooled flow boiling heat transfer to pure water and n-heptane in an annular heat exchanger*. Annals of Nuclear Energy, 53, 401-410 (2013). DOI: [10.1016/j.anucene.2012.07.037](https://doi.org/10.1016/j.anucene.2012.07.037)
- 31 Sarafraz M. M., Peyghambarzadeh S. M., Vaeli N., *Subcooled flow boiling heat transfer of ethanol aqueous solutions in vertical annulus space*. Chemical Industry and Chemical Engineering Quarterly, 18(2), 315-327 (2012). DOI: [10.2298/CICEQ111020008S](https://doi.org/10.2298/CICEQ111020008S)
- 32 Chen J. C., *A correlation for boiling heat transfer to saturated fluids in convective flow*. Industrial Engineering Chemistry Process Design Development, 5(3), 322-329 (1966). DOI: [10.1021/i260019a023](https://doi.org/10.1021/i260019a023)
- 33 Gungor K. E., Winterton H. S., *A general correlation for flow boiling in tubes and annuli*. International Journal of Heat and Mass Transfer, 29(3), 351-358 (1986).